Published in final edited form as:
Exp Cell Res. 2008 February 1; 314(3): 564–573.

Tropomyosin 4 Regulates Adhesion Structures and Resorptive Capacity in Osteoclasts

Brooke K. McMichael and **Beth S. Lee**
Department of Physiology and Cell Biology, The Ohio State University College of Medicine, Columbus, Ohio

Abstract

Tropomyosins (Tms) are α-helical dimers that bind and stabilize actin microfilaments while regulating their accessibility to other actin-associated proteins. Four genes encode expression of over forty Tms, most of which are expressed in nonmuscle cells. In recent years, it has become clear that individual Tm isoforms may regulate specific actin pools within cells. In this study, we examined how osteoclast function may be regulated by the tropomyosin isoform Tm-4, which we previously showed to be highly localized to podosomes and sealing zones of osteoclasts. RNAi-mediated knockdown of Tm-4, both in RAW264.7- and mouse marrow-derived osteoclasts, resulted in thinning of the actin ring of the sealing zone. Knockdown of Tm-4 also resulted in diminished bone resorptive capacity and altered resorption pit shape. In contrast, osteoclasts overexpressing Tm-4 demonstrated thickened podosomes on glass as well as thickened, aberrant actin structures on bone, and diminished motility and resorptive capacity. These results indicate that Tm-4 plays a role in regulating adhesion structures of osteoclasts, most likely by stabilizing the actin microfilaments present in podosomes and the sealing zone.

Keywords

tropomyosin; actin; motility; osteoclasts

INTRODUCTION

Osteoclasts are giant multinucleated cells of the monocyte-macrophage lineage that play a critical role in skeletal health by resorbing bone to be renewed in the remodeling process. This is achieved by the cells passing through cycles of migration, polarization coupled to bone resorption, depolarization and further migration. These highly motile cells express attachment structures called podosomes that are characterized by a short, rapidly assembling and disassembling F-actin core. This core contains actin regulatory proteins such as Arp2/3, Wasp, and gelsolin that regulate its structure and stability [1,2]. Surrounding the core are integrins and associated regulatory kinases, adaptors, small GTPases, and mediators of endocytosis [3], as well as a “cloud” of additional monomeric and filamentous actin that polymerizes and depolymerizes continuously [4]. Recently, this cloud has been shown to contain actin fibers that radiate perpendicular to the F-actin core [5]. While osteoclasts cultured on glass possess

Direct all correspondence to: Beth S. Lee, Ph.D., Department of Physiology and Cell Biology, The Ohio State University College of Medicine, 302 Hamilton Hall, 1645 Neil Avenue, Columbus, OH 43210, Tel: 614-688-3585, Fax: 614-292-4888, Email: lee.2076@osu.edu.

abundant numbers of individual podosomes, they are less prevalent in cells on bone [6]. Instead, podosomal proteins are configured into a dense adhesion structure termed the sealing zone, an actin-rich ring that surrounds a specialized membrane domain, the ruffled border. Secretion of degradative proteases (particularly cathepsin K) and protons (via proton-translocating VATPases) from the ruffled border results in degradation of bone matrix and dissolution of mineral. While the sealing zone contains the same regulatory proteins as podosomes, they are configured into a different three-dimensional structure, with sealing zones being thicker and denser than belts of podosomes [5,6].

Because the actin cytoskeleton of osteoclasts is highly dynamic, we examined these cells for the expression and distribution of tropomyosins. Tropomyosins are coiled-coiled dimers that bind along the length of actin filaments and stabilize their structures by regulating access of the filament to other actin regulatory proteins such as gelsolin [7], Arp2/3 [8], and ADF/cofilin [9,10]. Approximately forty isoforms of tropomyosins now have been identified in rodents, and most of these are expressed in nonmuscle cells [11]. We showed recently that at least seven isoforms are present in osteoclasts, and that one of these isoforms, tropomyosin 4 (Tm-4), was distributed both in the core of podosomes, and on the inner face of sealing zones [12]. Thus, Tm-4 appears to be a prime candidate for regulating osteoclast attachment and bone resorptive capacity. In this study, to identify a role for Tm-4 in osteoclast activity, we both inhibit and overexpress Tm-4 in murine osteoclasts, and assess resulting alterations in morphology, motility, and resorptive activity.

MATERIALS AND METHODS

Osteoclast culture

Murine osteoclasts were generated either from the macrophage cell line RAW264.7 (American Type Culture Collection, Manassas, VA) or from mouse bone marrow precursors. To generate RAW264.7-derived osteoclasts, macrophage precursors were plated at 20,000 cells/cm² and cultured for 5–8 days in Dulbecco's modified Eagle's medium (DMEM) containing 10% heat inactivated fetal bovine serum, penicillin/streptomycin and 50 ng/ml of a GST-RANKL fusion protein that was previously described [13], replacing the medium every 2–3 days. For the primary cell preparation, marrow cells from male Swiss-Webster mice (Harlan, Indianapolis, IN), 4–8 weeks in age, were incubated overnight in αMEM containing 10% heat inactivated fetal bovine serum and 20 ng/ml M-CSF (R & D Systems, Minneapolis, MN). The next day, non-adherent cells were collected and incubated for an additional 5–8 days in αMEM containing 10% heat inactivated fetal bovine serum, 20 ng/ml M-CSF, and 50 ng/ml GST-RANKL. The culture medium was replaced every 2–3 days.

Antibodies and Western analysis

For detection of Tm-4, a rabbit polyclonal was purchased from Chemicon International (Temecula, CA). Loading control antibodies to glyceraldehyde-3-phosphate dehydrogenase (GAPDH) and beta actin, both mouse monoclonal antibodies, were purchased from Abcam (Cambridge, MA). An antibody against V-ATPase subunit a3 was generated in this laboratory and was described previously [14]. Antibodies to paxillin and α-actinin were obtained from BD Transduction Laboratories and Sigma, respectively. For Western analysis, osteoclast lysates were run in pre-cast PAGE gels (Bio-Rad Laboratories, Hercules, CA) and transferred to Hybond membrane (GE Healthcare Bio-Sciences, Piscataway, NJ). Primary antibodies were allowed to bind to the membranes using standard methodology, and were detected using horseradish peroxidase-labeled secondary antibodies coupled with SuperSignal West Pico Chemiluminescent reagents (Pierce Biotechnology, Rockford, IL).

Competitive RT-PCR of Tm-4 mRNA

To determine Tm-4 mRNA expression levels by RT-PCR, primers were created that corresponded to sequences within the murine cDNA. The sense primer was of the sequence 5'-AGCCCCACACTTTGAAGCAC-3', while the antisense primer was of the sequence 5'-CCTGGAATAAGACGCTTGCTCC-3'. For an internal standard, a cDNA was created that corresponded to the expected PCR product using the primers above, but contained an internal deletion of 17%, a T7 promoter element, and a tail of 15 adenosines, as previously described [15,16]. This product was transcribed in vitro using the MAXIscript system (Ambion, Austin, TX), and 10 pg of the resulting RNA (the internal standard) was added to 1 μg of osteoclast total cellular RNA prior to reverse transcription and PCR. These reactions were performed using the Superscript First-strand Synthesis System and TaqDNA Polymerase, both from Invitrogen (Carlsbad, CA). The resulting RT-PCR products were run in a 2% agarose gel and stained with ethidium bromide to visualize the relative intensities of the bands. Quantification of bands was performed with a Chemi-doc supplied with Quantity One software (Bio-Rad Laboratories, Hercules, CA).

Immunocytochemistry and Microscopy

Osteoclasts were cultured either on glass coverslips or thinly-cut ivory slices. Cells briefly were fixed in a solution of 1% formaldehyde in pH 6.5 stabilization buffer (127 mM NaCl, 5 mM KCl, 1.1 mM NaH_2PO_4, 0.4 mM KH_2PO_4, 2 mM $MgCl_2$, 5.5 mM glucose, 1 mM EGTA, 20 mM Pipes), and subsequently were more extensively fixed and permeabilized in a solution of 2% formaldehyde, 0.2% Triton X-100, and 0.5% deoxycholate in the same stabilization buffer [12,17]. Primary antibodies were added in a standard blocking buffer, and were detected using Alexa-labeled secondary antibodies (Invitrogen Corp., Carlsbad, CA). F-actin was identified using Alexa-labeled phalloidin, also from Invitrogen. Cells were visualized using a Zeiss 510 META laser scanning confocal microscope (Campus Microscopy and Imaging Facility, The Ohio State University). Actin ring and podosome thicknesses were determined by generating Z-stack images of randomly selected cells and measuring these structures at their thickest points.

Knockdown and overexpression of Tm-4

To knock down murine Tm-4 expression, siRNAs were designed and synthesized by Ambion (Austin, TX). Most experiments were performed with siRNA1, which was of the sequence 5'-CCCAGAGCAAAAAUUAACAtt-3' (sense) and 5'-UGUUAAUUUUUGCUCUGGGtg-3' (antisense). Optimization experiments were performed and showed this siRNA to work efficiently at 75 nM. Confirmatory experiments were performed with siRNA2 (at 100 nM), which was of the sequence 5'-CCUACUCUGUUCUUUACGUtt-3' (sense) and 5'-ACGUAAAGAACAGAGUAGGtt-3' (antisense). These oligonucleotides target sequences within the 3' UTR of the Tm-4 mRNA. Because Tm-4 is the sole product of the Tmδ gene, the siRNA sequences bears no homology to other known Tm isoforms. Assay of the isoforms Tm-2/3, Tm-5a/5b, and 5NM-1, which also are abundant in osteoclasts, showed no diminution when cells were treated with the Tm-4 siRNA (data not shown). RAW264.7 cells were transfected by first stimulating with GST-RANKL to form osteoclasts. On day 5 of GST-RANKL treatment, a solution of siRNA or a non-targeting control dsRNA at the same concentration (Ambion) was added to Lipofectamine 2000 (Invitrogen Corp., Carlsbad, CA) in plain DMEM without serum or antibiotics and added to the cells. The medium was replaced with DMEM with fetal bovine serum and RANKL but no antibiotics after five hours [18]. At 1–3 days post-transfection, cells were harvested as required. Transfection efficiency, as measured by introduction of a commercial fluorescent dsRNA (Sequitur/Invitrogen Corp.) was >95% in multinucleated cells. For immunocytochemical analysis, the cells were scraped and

replated on ivory slices or glass coverslips immediately following the transfection. For RNA and protein analysis, total cellular RNA was harvested with RNA-Bee (Tel-test, Inc., Friendswood, TX), and whole cell lysates for protein assays were harvested using M-PER (Pierce Biotechnology, Rockford, IL).

Bone marrow-derived osteoclasts were transfected via electroporation. On day five of GST-RANKL treatment, after osteoclasts had formed, cells were scraped, pelleted, and resuspended in siPORT buffer (Ambion, Austin, TX). The cells were electroporated at 250V/ 50μF with siRNA or non-targeting control dsRNA, then plated in standard differentiation medium on glass or ivory for immunocytochemistry, or plastic for RNA and protein analysis. As for RAW264.7 osteoclasts, transfection efficiency was assayed with a fluorescent dsRNA and found to be >95%.

For generation of a Tm-4 expression plasmid, an I.M.A.G.E. clone corresponding to the murine form (accession number BC023701) was purchased from the American Type Culture Collection (Manassas, VA). A fragment containing 19 bp of 5' UTR, the entire coding region, and 32 bp of the 3' UTR was subcloned into the eukaryotic expression vector pEF6/V5-His (Invitrogen Corp., Carlsbad, CA). This construct was stably transfected into RAW264.7 macrophages; the empty pEF6/V5-His vector was stably transfected into cells as a control via Lipofectamine and Plus reagent transfections (Invitrogen Corp., Carlsbad, CA). Cells were maintained in 3 μg/ml blasticidin for selection.

Osteoclast resorption and motility assays

Five days after initial RANKL stimulation, osteoclasts were transfected and immediately plated on BD BioCoat Osteologic Discs (BD Biosciences, San Jose, CA). Control and siRNA treated cells were kept on the discs for 3 days. Alternately, Tm-4 overexpressing cells were cultured on the discs for up to 8 days. The cells were removed by the addition of bleach for 5 minutes and several washes with water. Resorbed areas (clearings) were assayed by photographing the resulting discs under low magnification, and quantifying these areas with SigmaScan Pro 5.0 software (SPSS Science, Chicago, IL) as previously described [19]. Equal numbers of images were compared among test groups. Groups were assayed for number of clearings, area per clearing, and total resorption.

Motility was measured by the use of 8.0 μm pore Transwell migration chambers (Corning Life Sciences, Acton, MA). The bottom side of the membrane was coated with collagen (3 mg/ml diluted 1:2 with 100% ethanol) and dried overnight. Five days after RANKL stimulation or immediately following transfection of RAW or marrow cells, cells were scraped and replated on the upper side of the membrane. After 48 hours, the cells were stimulated overnight to migrate by the addition of 40 μg/ml osteopontin peptide to the bottom of the well. Cells on the upper side of the membrane were removed with a cotton swab, and the remaining cells were fixed and stained for tartrate resistant acid phosphatase using a Leukocyte Acid Phosphatase kit (Sigma, St. Louis, MO).

RESULTS

Suppression of tropomyosin 4 levels results in thinning of the osteoclast F-actin ring

We previously showed that tropomyosin 4 is abundant in osteoclast adhesion structures, namely on the inner face of both the podosomal F-actin core and the F-actin ring of polarized osteoclasts [12]. Based on these data, we hypothesized a role for Tm-4 in stabilizing both podosomal and sealing zone microfilaments. To further explore a role for Tm-4 in regulating the actin cytoskeleton of osteoclasts, we used RNA interference to suppress its expression levels, and examined the cells for changes in actin architecture and bone resorptive capacity.

Tm-4 is the only product of the Tmδ gene, and therefore is readily amenable to genetic manipulation by RNA interference. Two siRNAs tested demonstrated significant knockdown of Tm-4; siRNA1 was used for most experiments while siRNA2 was used to confirm specificity of these results as described below. Figure 1 shows that Tm-4 mRNA and protein levels successfully were suppressed in both RAW264.7- and marrow-derived osteoclasts with siRNA1. In panel 1A, siRNA- or control-transfected RAW264.7 osteoclasts were analyzed by competitive RT-PCR for Tm-4 mRNA levels. We saw significant mRNA knockdown by one day post-transfection, and these low levels remained until at least three days post-transfection (compare the intensities of the upper Tm-4 bands to the lower internal standards). Tm-4 protein levels also diminished by one day post-transfection, and remained low through the same time period (Figure 1B). In contrast, expression of housekeeping genes such as GAPDH did not change, nor did the expression of β-actin. Figure 1C shows quantification of siRNA effects on Tm-4 expression and demonstrates ~50% loss of both mRNA and protein over the three day assay period. Comparable results were obtained in murine marrow-derived osteoclasts, as shown in panels 1D–1F, demonstrating the similarity of these culture models. The effects of siRNA2 on Tm-4 also were assessed; at 100 nM, this oligonucleotide also generated a ~50% decrease in Tm-4 mRNA levels and a ~45% decrease in protein levels (data not shown). Although only ~50% knockdown was achieved in either cell type and with either siRNA, control experiments demonstrated >95% transfection efficiency in osteoclasts (see Materials and Methods). Immunocytochemical staining revealed uniform suppression of Tm-4 among osteoclasts in the siRNA-treated culture, rather than, for example, 100% suppression in one-half the cells. Figure 1G illustrates that control-transfected osteoclasts produced intense Tm-4 labeling at the peripheral podosome belt (left panels); in contrast, while some siRNA-treated mononuclear cells still showed intense Tm-4 labeling, siRNA-treated osteoclasts uniformly were diminished in intensity when photographed under the same conditions as controls (right panels).

To determine how suppression of Tm-4 might affect F-actin structures in osteoclasts, we performed confocal imaging of RAW264.7- or marrow-derived cells cultured on ivory and labeled with fluorescent phalloidin. Although osteoclasts were able to generate sealing zones in the siRNA-treated cells, Z-stack imaging revealed that the height of F-actin rings in these cells was significantly less than in control-treated or wild-type cells. Figure 2A shows representative photomicrographs of control-transfected and siRNA1-transfected osteoclasts. As indicated by the arrowheads, siRNA1-treated cells contained much thinner actin rings than their control-transfected counterparts. To quantify these results, actin rings from untransfected, controltransfected, and siRNA1-transfected osteoclasts were measured at their thickest points, and these data were expressed graphically in Figure 2B. These results were obtained from a single experimental batch of cells; however, nearly identical results were obtained from three other trials. As is apparent from this graph, siRNA1 treatment of both RAW264.7- and marrow-derived cells resulted in diminution of actin ring thickness by 40–50%. Similarly, treatment with siRNA2 generated actin rings that were diminished in thickness by ~45% (data not shown). These results are consistent with a role for Tm-4 in stabilizing actin filaments within the osteoclast sealing zone.

Although native tissue like ivory is the most physiologically authentic substrate on which to grow bone cells, the rather irregular surface and opacity of ivory may cause artifacts in fluorescent imaging, which could skew our measurements of sealing zone height. To control for this possibility, we performed similar experiments with osteoclasts plated on thinly coated synthetic bone surface (BD BioCoat Osteologic coverslips). As shown in Figure 2C and 2D, nearly identical results were obtained with this substrate, furthering confirming our findings that suppressed Tm-4 levels affect sealing zone formation.

Suppression of Tm-4 levels results in impaired bone resorption and motility

The altered formation of osteoclast sealing zones in cells with suppressed Tm-4 levels suggested that these osteoclasts may not be able to resorb bone in a normal manner. To determine the resorptive capacity of these cells, control- and siRNA-transfected RAW264.7 osteoclasts were plated on synthetic bone substrate and the number and area of resulting clearings were quantified. As shown in Figure 3A (top), both the number and size of individual clearings were diminished in siRNA-transfected cells relative to control-transfected controls, for a loss in total resorption of about 80%. This was not due to differences in cell number between the control- and siRNA-treated cells, since equivalent numbers of differentiated osteoclasts were transfected in each sample. Resorption assays from marrow-derived cells similarly demonstrated a roughly 60% decrease in total resorption (not shown). Further, the shapes of resorbed areas generated by the knockdown cells were altered; they were irregular in shape, and often showed patches of incomplete resorption within the clearings themselves (Figure 3A, bottom, arrowheads). In contrast, clearings generated by the control-transfected cells generally were complete and rounded in outline, resembling the resorption areas generated by wild-type cells on Osteologic discs [20]. Because irregular resorption areas might be indicative of aberrant motility in the knockdown cells, Transwell migration assays were performed. As shown in Figure 3B, addition of siRNA to cells resulted in a 50% loss in motility. These results suggest a potential alteration in cytoskeletal organization. Although we did not discern obvious morphological differences in podosome structure, we found that siRNA-treated cells that were plated on glass showed regions of long actin filaments resembling stress fibers in regions where Tm-4 was relatively absent (Figure 3C, arrowheads). This is in contrast to wild-type or control-transfected osteoclasts, which do not contain stress fibers [21]. Thus, loss of F-actin from normal osteoclast adhesion structures resulted in formation of aberrant microfilament organization.

Overexpression of tropomyosin 4 results in altered F-actin structures in osteoclasts

Because suppression of Tm-4 alters the ability of osteoclasts to generate actin rings and resorb bone, we explored whether overexpression of this isoform could similarly disrupt osteoclast activity. Stably transfected RAW264.7 cell macrophage lines were generated containing either Tm-4 cDNA in vector pEF6/V5-His or empty vector as a control, and these lines subsequently were differentiated into osteoclasts. (Expression of Tm-4 in this vector is driven by the promoter for human elongation factor 1α) Figure 4A shows Western analysis of several of these clones, which expressed up to 2-fold more Tm-4 than untreated or control-transfected cells. Clones 1.1, 1.2, and 2.2 were chosen for detailed analyses. Other experiments (not shown) using the stronger CMV promoter to express Tm-4 resulted in complete cell death, indicating that macrophages and osteoclasts may not be able to tolerate large deviations in levels of this tropomyosin. Figure 4B demonstrates that even the highest expressing of our stable clones (Tm- 4 1.1) was able to generate osteoclasts, and did so at a frequency approximately 91% of that of the control line (not shown). However, even a small increase in Tm-4 expression resulted in aberrant actin structures. F-actin labeling of podosomes appeared more intense in Tm-4-transfected osteoclasts than in control cells. Further, many of the Tm-4 overexpressing cells demonstrated intense phalloidin labeling of podosomes scattered across the cell base, rather than being arranged in a peripheral belt (Figure 4B). Although clone 1.1 is shown, overexpressing clones 1.2 and 2.2 demonstrated a similar phenotype (not shown).

The F-actin structures in Tm-4 overexpressing cells gave the appearance of podosomes from phalloidin labeling; however, we performed additional immunocytochemistry to determine whether podosome-associated proteins were present in these structures. The left panels of Figure 4C show that α-actinin, which associates with the actin core of podosomes under normal conditions [22], also intensely labels the F-actin structures in Tm-4-overexpressing cells. Another podosome-associated protein, paxillin, is present in the cloud which surrounds the

actin core in wild-type cells, and in mature podosome belts, can elicit a railroad track appearance due to its distribution at the periphery of densely packed cores [23]. A similar distribution is apparent in our control transfectants (Figure 4C, right panels). However, in Tm-4- overexpressing cells with scattered individual podosome-like structures, paxillin is distributed throughout the cell and can be seen surrounding the thickest actin cores (Figure 4C, arrows). Thus, in cells overexpressing Tm-4, α-actinin colocalizes with the cores of the thickened F-actin structures while paxillin surrounds them; these patterns are consistent with the identity of the structures as podosomes.

To determine whether the intense phalloidin labeling of podosomes in the overexpressing lines was due to increased F-actin in the podosomal cores, Z-stack images of control and overexpressing cells (clone 1.1) were generated and core actin height was measured (Figure 4D).Because the height of podosomes (~1μm) is near the optical resolution of confocal microscopes, the values generated are not extremely precise; nonetheless, it was clear that the height of podosomes of Tm-4 overexpressing cells (range, 3.0 – 4.0 microns) was greater than those of control-treated cells (range, 1.0 – 2.5 microns). Transwell migration assays were then performed on osteoclasts of clone 1.1 to determine whether Tm-4 overexpressers were altered in their motility. As demonstrated in Figure 4E, overexpression of Tm-4 resulted in a 65% loss of cell motility under our assay conditions.

When plated on an ivory substrate, the Tm-4 overexpressing cells (both clone 1.1 and clone 2.2) produced even more aberrant attachment structures. While cells expressing the control vector were able to polarize properly on ivory, we found that Tm-4 overexpressing cells were unable to form sealing zones, and many of these cells produced globular patches of F-actin that surrounded the periphery of the cells, and were particularly apparent at the cell base where the sealing zone is formed under normal conditions (Figure 5A). In some of the Tm-4 overexpressing cells, structures with the appearance of very small actin rings were generated, as indicated by the arrow in Figure 5A.

The sealing zone of normal osteoclasts surrounds the ruffled border, which contains an abundance of V-ATPase complexes. V-ATPases are proton-translocating transporters that become enriched in ruffled borders of polarized osteoclasts and mediate acidification of the resorptive space [24,25]. A lack of V-ATPases in the ruffled border results in impaired bone resorption, and in humans and mouse models, a malignant form of osteopetrosis [26–29]. Figure 5B shows confocal sections at the base of either a control-transfected (top panels) or Tm-4 overexpressing (bottom panels) cell. Both cells are labeled for F-actin and the a3 subunit of the V-ATPase, a subunit isoform that is highly enriched in the ruffled border [30]. As demonstrated, the lack of actin rings in the overexpressing cells corresponds with a lack of ruffled border V-ATPases. This was not due to a defect in V-ATPase expression, since a3 levels in the Tm-4 overexpressing cells was not altered (data not shown). Not unexpectedly, bone resorption by the Tm-4 overexpressing cells was severely impaired. Under our normal assay conditions, osteoclasts of clone 1.1 exhibited no resorption when on either Osteologic discs or ivory slices for a standard assay period of three days (not shown). However, when cells were plated and differentiated on Osteologic discs for an unusually long period of eight days, a small amount of resorption was noted (Figure 5C). These results together suggest that minimal overexpression of Tm-4 causes abnormal stabilization and thickening of osteoclast microfilaments, particularly in cell attachment structures where Tm-4 is normally abundant.

DISCUSSION

These studies demonstrate that tropomyosin 4 plays a critical role in regulation of osteoclast attachment structures, and consequently, osteoclast function. This work represents the first report of tropomyosin function in podosomal-based adhesion complexes, and one of the first

reports in which a specific tropomyosin isoform is assigned a distinct function within a cell. Our previous studies characterized the distribution of multiple tropomyosin isoforms within osteoclasts, and only Tm-4 was shown to associate with the F-actin core of podosomes and to form a cap over the inner face of the sealing zone. In addition, Tm-5a and/or -5b also were shown to be associated with podosomes, but these isoform(s) were found to surround the core and be more heavily associated with the outer edges of the sealing zone than to cap the entire inner face. Thus, it seems likely that these isoforms, in addition to Tm-4, will play distinct roles in regulating F-actin structures involved in osteoclast attachment and motility. Experiments to identify a role for Tm-5a and Tm-5b are underway.

Our findings in this and the previous study are consistent with Tm-4 playing a role in stabilizing both podosomal and sealing zone actin filaments. In both cases, this tropomyosin was found in the inner faces of these structures [12], and we propose that Tm-4 is likely to stabilize these actin filaments by regulating access of other proteins that may play roles in actin turnover. Our knockdown and overexpression studies are consistent with this hypothesis; lower Tm-4 levels result in thinning of sealing zones while overexpression resulted in thickened podosome filaments and thickened but disrupted actin structures in osteoclasts on bone. Indeed, it appears that Tm-4 levels may be limiting for assembly of these adhesion structures. While inhibition of Tm-4 also may cause thinning of podosomes, we were unable to generate measurements of these structures due to the optical resolution of confocal microscopes. Nonetheless, our results suggest that disruption of the attachment structures by either under- or over-expression resulted in aberrant bone resorption and motility. It appears that osteoclasts were able to tolerate little alteration in Tm-4 levels in either direction; we were able to knock down expression by only about 50% or increase expression by about 2-fold. Attempts to increase overexpression levels further with the use of viral promoters resulted in complete cell death. These results are perhaps not surprising, given the fundamental role of the actin cytoskeleton in cell adhesion, motility, and cell division. Our inability to completely abolish Tm-4 may reflect the fact that at least some amount of this protein is required for podosome/sealing zone formation, and thus, cell attachment.

Tropomyosin 4 is expressed at equal levels in osteoclasts and macrophages, which also form podosomes but do not generate sealing zones. We found previously that Tm-4 was expressed at similar levels in fibroblasts, which generate focal adhesions and stress fibers, but not podosomes or sealing zones [12]. Other studies of Tm-4 levels in whole tissues showed that this isoform was expressed at relatively high levels in kidney, liver, lung, spleen, and stomach in addition to embryonic fibroblasts. Expression was lower in brain and heart, and undetectable in muscle [31], although other studies have shown this isoform to be present in both skeletal and cardiac muscle [32]. Therefore, Tm-4 can be utilized for the stabilization of microfilament structures other than podosomes and sealing zones, depending on the cell type. However, this isoform may play a general role in motile events. Tm-4 is found primarily in growth cones of developing neurons [33,34], and is upregulated as contractile smooth muscle cells dedifferentiate into noncontractile, migrating cell types [32]. Unfortunately, potential studies of Tm-4 in many other tissues are hindered by the fact that available antibodies can cross-react with higher molecular weight isoforms that are not expressed by macrophages and osteoclasts, but are present in numerous other cell types [31,34].

In summary, Tm-4 appears to regulate osteoclast motility and bone resorption by stabilizing actin filaments within podosomes and the sealing zone. Minimal changes in Tm-4 expression, either to lowered or heightened levels, cause significant alterations in the structure and functionality of these attachment structures. By virtue of tropomyosins' abilities to regulate access to actin modifying proteins such as gelsolin and ADF/cofilin, they play an important role in maintenance of microfilament dynamics. Although the mechanisms regulating interactions between actin filaments and nonmuscle tropomyosins are not well understood,

these results confirm that Tm isoforms can segregate to specific subcellular domains and mediate local microfilament structure and function.

ACKNOWLEDGEMENTS

This work was supported by NIH AR051515 and DK0512131 (to BSL) and The Ohio State University. The authors would like to thank Dr. Richard Burry and the Campus Microscopy and Imaging Facility at The Ohio State University for technical advice and support.

REFERENCES

1. Linder S, Aepfelbacher M. Podosomes: adhesion hot-spots of invasive cells. Trends Cell Biol 2003;13:376–385. [PubMed: 12837608]
2. Linder S, Kopp P. Podosomes at a glance. J Cell Sci 2005;118:2079–2082. [PubMed: 15890982]
3. Jurdic P, Saltel F, Chabadel A, Destaing O. Podosome and sealing zone: specificity of the osteoclast model. Eur J Cell Biol 2006;85:195–202. [PubMed: 16546562]
4. Destaing O, Saltel F, Geminard JC, Jurdic P, Bard F. Podosomes display actin turnover and dynamic self-organization in osteoclasts expressing actin-green fluorescent protein. Mol Biol Cell 2003;14:407–416. [PubMed: 12589043]
5. Luxenburg C, Geblinger D, Klein E, Anderson K, Hanein D, Geiger B, Addadi L. The architecture of the adhesive apparatus of cultured osteoclasts: from podosome formation to sealing zone assembly. PLoS ONE 2007;2:e179. [PubMed: 17264882]
6. Saltel F, Destaing O, Bard F, Eichert D, Jurdic P. Apatite-mediated actin dynamics in resorbing osteoclasts. Mol Biol Cell 2004;15:5231–5241. [PubMed: 15371537]
7. Ishikawa R, Yamashiro S, Matsumura F. Differential modulation of actin-severing activity of gelsolin by multiple isoforms of cultured rat cell tropomyosin. Potentiation of protective ability of tropomyosins by 83-kDa nonmuscle caldesmon. J Biol Chem 1989;264:7490–7497. [PubMed: 2540194]
8. Blanchoin L, Pollard TD, Hitchcock-DeGregori SE. Inhibition of the Arp2/3 complex-nucleated actin polymerization and branch formation by tropomyosin. Curr Biol 2001;11:1300–1304. [PubMed: 11525747]
9. Bernstein BW, Bamburg JR. Tropomyosin binding to F-actin protects the F-actin from disassembly by brain actin-depolymerizing factor (ADF). Cell Motil 1982;2:1–8. [PubMed: 6890875]
10. Ono S, Ono K. Tropomyosin inhibits ADF/cofilin-dependent actin filament dynamics. J Cell Biol 2002;156:1065–1076. [PubMed: 11901171]
11. Gunning PW, Schevzov G, Kee AJ, Hardeman EC. Tropomyosin isoforms: divining rods for actin cytoskeleton function. Trends Cell Biol 2005;15:333–341. [PubMed: 15953552]
12. McMichael BK, Kotadiya P, Singh T, Holliday LS, Lee BS. Tropomyosin isoforms localize to distinct microfilament populations in osteoclasts. Bone 2006;39:694–705. [PubMed: 16765662]
13. Krits I, Wysolmerski RB, Holliday LS, Lee BS. Differential localization of myosin II isoforms in resting and activated osteoclasts. Calcif Tissue Int 2002;71:530–538. [PubMed: 12232674]
14. Manolson MF, Yu H, Chen W, Yao Y, Li K, Lees RL, Heersche JN. The a3 isoform of the 100-kDa V-ATPase subunit is highly but differentially expressed in large (≥10 nuclei) and small (≤5 nuclei) osteoclasts. J Biol Chem 2003;278:49271–49278. [PubMed: 14504271]
15. Jeyaraj S, Dakhlallah D, Hill SR, Lee BS. HuR stabilizes V-ATPase mRNA during cellular energy depletion. J. Biol. Chem 2005;280:37957–37964. [PubMed: 16155006]
16. Lee BS, Holliday LS, Krits I, Gluck SL. Vacuolar H^+-ATPase activity and expression in mouse bone marrow cultures. J. Bone Miner. Res 1999;14:2127–2136. [PubMed: 10620072]
17. Zeng Q, Lagunoff D, Masaracchia R, Goeckeler Z, Cote G, Wysolmerski R. Endothelial cell retraction is induced by PAK2 monophosphorylation of myosin II. J Cell Sci 2000;113(Pt 3):471–482. [PubMed: 10639334]
18. Hurst IR, Zuo J, Jiang J, Holliday LS. Actin-related protein 2/3 complex is required for actin ring formation. J Bone Miner Res 2004;19:499–506. [PubMed: 15040839]
19. Khadeer MA, Sahu SN, Bai G, Abdulla S, Gupta A. Expression of the zinc transporter ZIP1 in osteoclasts. Bone 2005;37:296–304. [PubMed: 16005272]

20. Valverde P, Tu Q, Chen J. BSP and RANKL induce osteoclastogenesis and bone resorption synergistically. J Bone Miner Res 2005;20:1669–1679. [PubMed: 16059638]

21. Warshafsky B, Aubin JE, Heersche JN. Cytoskeleton rearrangements during calcitonin-induced changes in osteoclast motility in vitro. Bone 1985;6:179–185. [PubMed: 4040768]

22. Marchisio PC, Cirillo D, Teti A, Zambonin-Zallone A, Tarone G. Rous sarcoma virus-transformed fibroblasts and cells of monocytic origin display a peculiar dot-like organization of cytoskeletal proteins involved in microfilament-membrane interactions. Exp Cell Res 1987;169:202–214. [PubMed: 3028844]

23. Pfaff M, Jurdic P. Podosomes in osteoclast-like cells: structural analysis and cooperative roles of paxillin, proline-rich tyrosine kinase 2 (Pyk2) and integrin alphaVbeta3. J Cell Sci 2001;114:2775–2786. [PubMed: 11683411]

24. Blair HC, Teitelbaum SL, Ghiselli R, Gluck S. Osteoclastic bone resorption by a polarized vacuolar proton pump. Science 1989;245:855–857. [PubMed: 2528207]

25. Väänänen HK, Karhukorpi EK, Sundquist K, Wallmark B, Roininen I, Hentunen T, Tuukkanen J, Lakkakorpi P. Evidence for the presence of a proton pump of the vacuolar H(+)-ATPase type in the ruffled borders of osteoclasts. J Cell Biol 1990;111:1305–1311. [PubMed: 2144003]

26. Kornak U, Schulz A, Friedrich W, Uhlhaas S, Kremens B, Voit T, Hasan C, Bode U, Jentsch TJ, Kubisch C. Mutations in the a3 subunit of the vacuolar H(+)-ATPase cause infantile malignant osteopetrosis. Hum. Mol. Gen 2000;9:2059–2063. [PubMed: 10942435]

27. Frattini A, Orchard PJ, Sobacchi C, Giliani S, Abinun M, Mattsson JP, Keeling DJ, Andersson AK, Wallbrandt P, Zecca L, Notarangelo LD, Vezzoni P, Villa A. Defects in TCIRG1 subunit of the vacuolar proton pump are responsible for a subset of human autosomal recessive osteopetrosis. Nat Genet 2000;25:343–346. [PubMed: 10888887]

28. Li Y, Chen W, Liang Y, Li E, Stashenko P. Atp6i-deficient mice exhibit severe osteopetrosis due to loss of osteoclast-mediated extracellular acidification. Nat Genet 1999;23:447–451. [PubMed: 10581033]

29. Scimeca JC, Franchi A, Trojani C, Parrinello H, Grosgeorge J, Robert C, Jaillon O, Poirier C, Gaudray P, Carle GF. The gene encoding the mouse homologue of the human osteoclast-specific 116-kDa V-ATPase subunit bears a deletion in osteosclerotic (oc/oc) mutants. Bone 2000;26:207–213. [PubMed: 10709991]

30. Toyomura T, Murata Y, Yamamoto A, Oka T, Sun-Wada GH, Wada Y, Futai M. From lysosomes to the plasma membrane: localization of vacuolar-type H+ -ATPase with the a3 isoform during osteoclast differentiation. J. Biol. Chem 2003;278:22023–22030. [PubMed: 12672822]

31. Schevzov G, Vrhovski B, Bryce NS, Elmir S, Qiu MR, O'Neill GM, Yang N, Verrills NM, Kavallaris M, Gunning PW. Tissue-specific tropomyosin isoform composition. J Histochem Cytochem 2005;53:557–570. [PubMed: 15872049]

32. Abouhamed M, Reichenberg S, Robenek H, Plenz G. Tropomyosin 4 expression is enhanced in dedifferentiating smooth muscle cells in vitro and during atherogenesis. Eur J Cell Biol 2003;82:473–482. [PubMed: 14582535]

33. Had L, Faivre-Sarrailh C, Legrand C, Mery J, Brugidou J, Rabie A. Tropomyosin isoforms in rat neurons: the different developmental profiles and distributions of TM-4 and TMBr-3 are consistent with different functions. J Cell Sci 1994;107(Pt 10):2961–2963. [PubMed: 7876361]

34. Hannan AJ, Gunning P, Jeffrey PL, Weinberger RP. Structural compartments within neurons: developmentally regulated organization of microfilament isoform mRNA and protein. Mol Cell Neurosci 1998;11:289–304. [PubMed: 9698395]

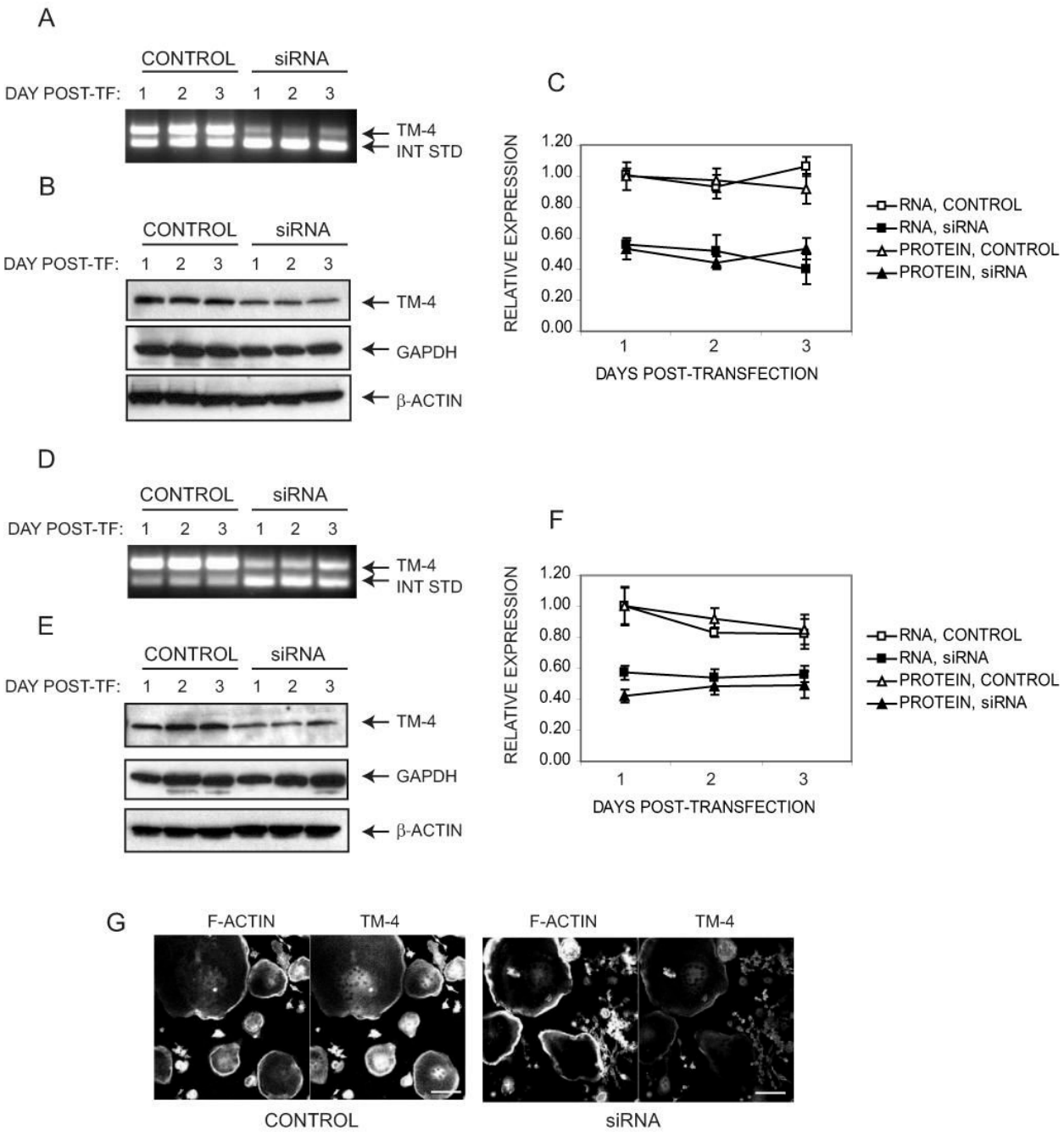

Figure 1. Suppression of tropomyosin 4 levels in osteoclasts

A, Competitive RT-PCR was performed on mRNA from control- or siRNA1-transfected RAW264.7 osteoclasts at 1, 2, or 3 days post-transfection. The upper band represents Tm-4 mRNA, while the lower band is an internal standard as described in Materials and Methods. *B*, Western analysis was performed on control-or siRNA1-treated RAW264.7 osteoclasts at 1, 2, or 3 days post-transfection. *C*, Data from experiments as shown in panels A and B were compiled, and the relative expression levels of Tm-4 mRNA and protein were compared in control and siRNA1-treated cells. At least three separate experiments were performed for each data set. Data points represent mean ± s.d. *D*, Competitive RT-PCR was performed as in panel *A*, but on control- or siRNA1-transfected mouse marrow-derived osteoclasts. *E*, Western

analysis was performed as in panel *B*, but on control- or siRNA1-transfected marrow derived osteoclasts. *F*, Data from marrow-derived osteoclasts were compiled and are presented similarly to the data shown in panel C. *G*, Cells from control- or siRNA-transfected cultures were double-labeled with phalloidin and an antibody against Tm-4. SiRNA-transfected osteoclasts show a uniform diminution in Tm-4 labeling. Scale bar = 100 μm.

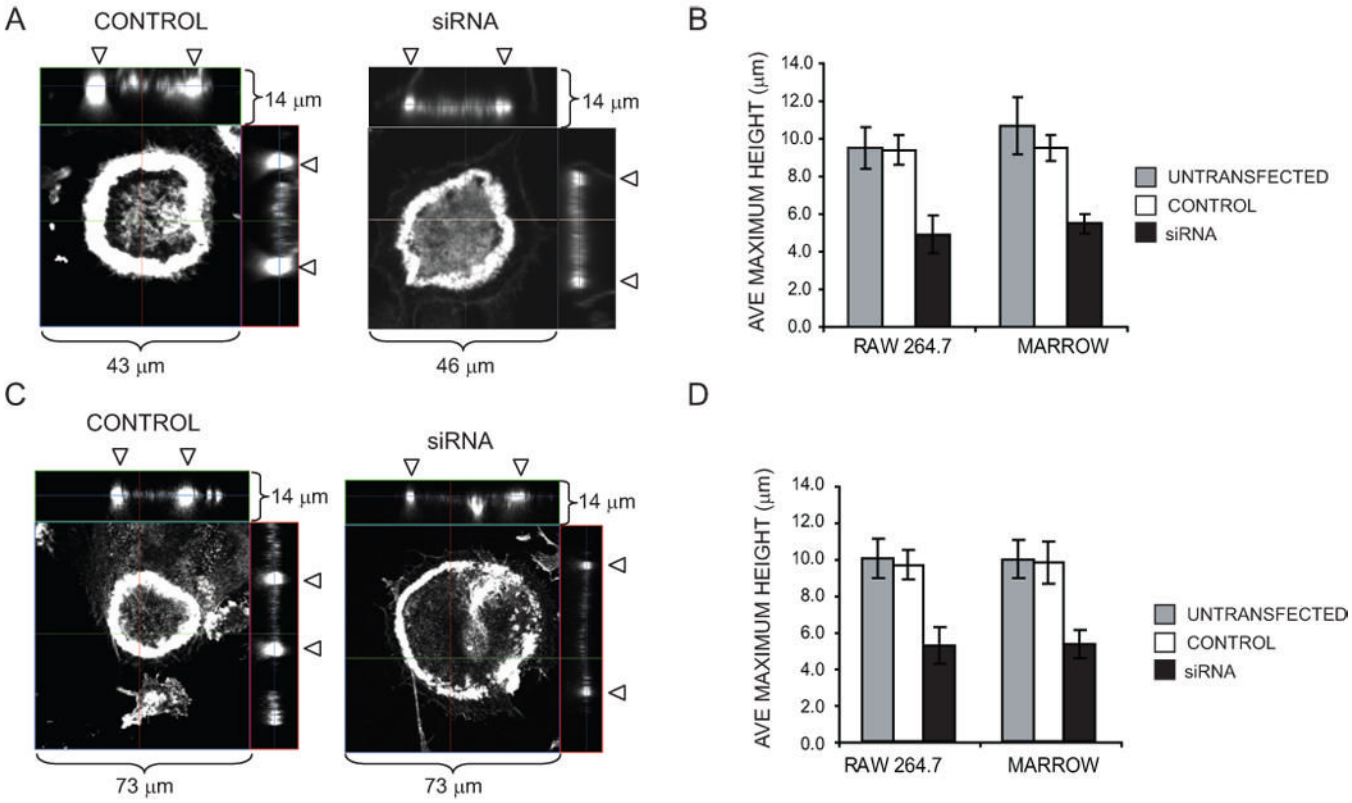

Figure 2. Loss of tropomyosin 4 results in thinning of the osteoclast sealing zone

Z-sections showing phalloidin labeling in control-or siRNA1-transfected cells were obtained from both osteoclasts plated on ivory (panel *A*) or a synthetic bone substrate (panel *C*). Arrows indicate the thickest regions of actin rings. The maximum heights of the sealing zones of transfected and untransfected cells, as plated on ivory (panel B) or synthetic substrate (panel D) were quantified and averaged. At least ten data points were taken for each group. Bars indicate mean ± s.d. In comparison of siRNA treatment versus untransfected or control-transfected cells by Student's t-test, $P < 0.0001$ for both RAW264.7 and marrow cells. Similar results were generated with siRNA2 (data not shown).

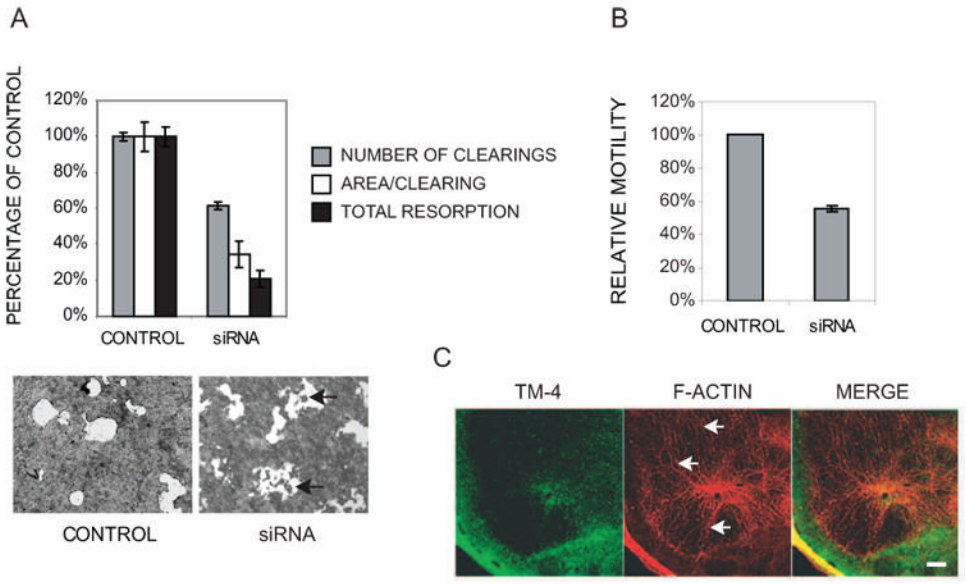

Figure 3. Loss of tropomyosin 4 diminishes bone resorption and motility by osteoclasts

A(top) Control- or siRNA-transfected RAW264.7 osteoclasts were plated on synthetic bone substrates, and the number of clearings, area of the clearings, and total resorption were quantified. At least 150 clearings were counted for each sample in each experiment. Graph indicates the mean ± s.d. from three independent experiments. For each comparison of control versus siRNA-treated cells, $P < 0.05$ by Student's t-test. (Bottom) Photomicrographs of resorption areas are shown, demonstrating the ragged shape of clearings from siRNA-transfected cells. Arrowheads indicate regions of incomplete resorption within these regions. The siRNA sample was photographed in a region of higher than average resorption in order to demonstrate multiple examples of irregularly shaped clearings. *B*, The motility of control- and siRNA-transfected osteoclasts was determined using Transwell migration assays. In three separate experiments, at least 950 migrated cells were counted for both control- and siRNA-transfected cells. The means from three experiments ± s.d. are shown; $P < 0.001$ by Student's t-test. *C*, An siRNA-transfected osteoclast pl regions of low Tm-4, is shown (arrowheads). Scale bar = 10 μm.

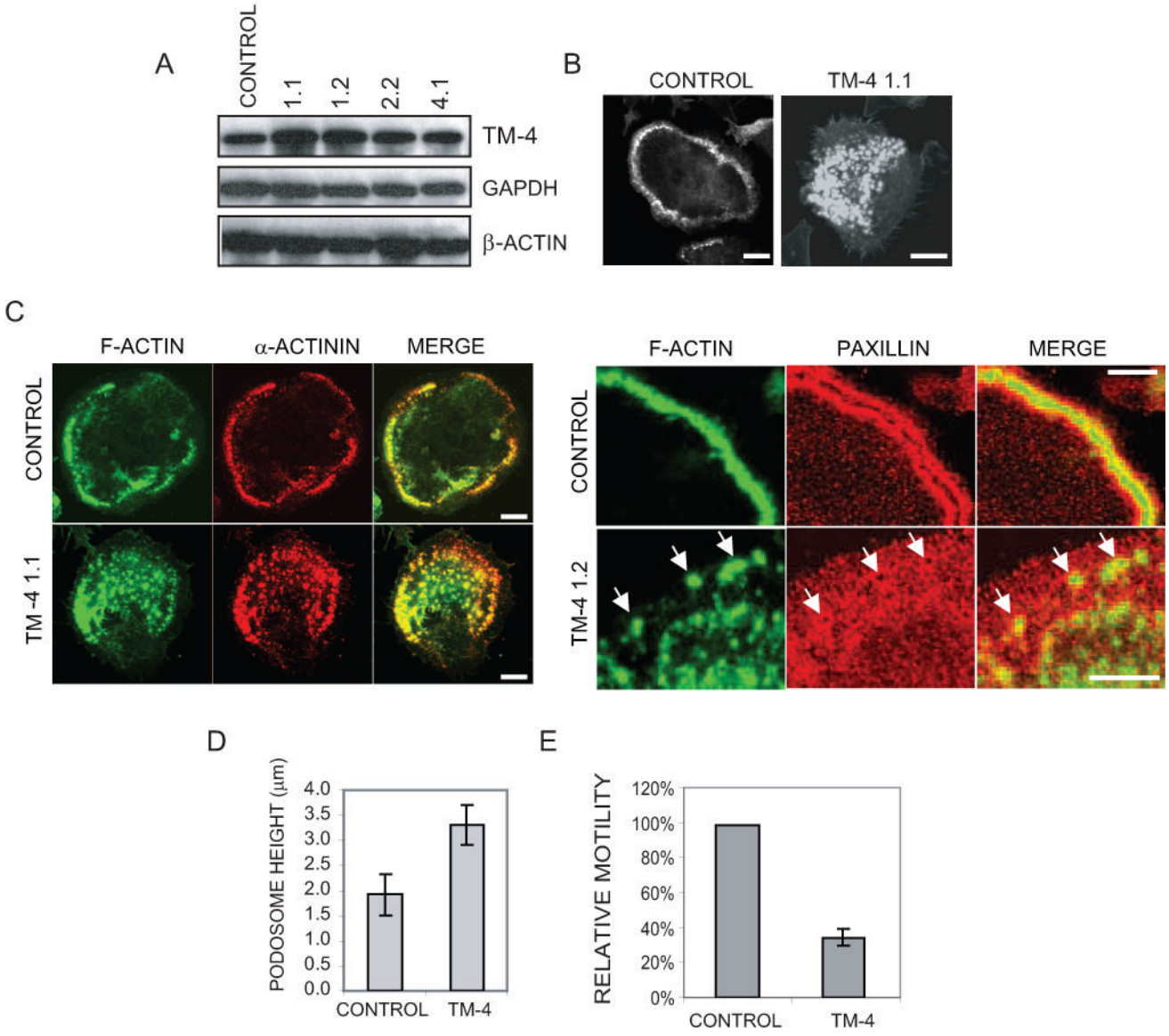

Figure 4. Overexpression of tropomyosin 4 results in thickened podosomes and loss of motility

A Western analysis of four Tm-4 overexpressing cell lines with an empty vector control line is shown. Blots of GAPDH and β-actin are included as loading controls. *B* Confocal micrographs of the stably transfected control cell line and Tm-4 overexpressing line 1.1 are stained for F-actin. While the control line is capable of forming podosome belts, the overexpressers often show clusters of thickened podosomes across the base of the cell. *C*(left), Control and Tm-4 overexpressing cells were doubly labeled for F-actin and α-actinin. (Right), Control and overexpressing cells were doubly labeled for F-actin and paxillin. Arrows indicate paxillin distribution around F-actin cores. Scale bars = 10 μm. *D*, Podosome height was measured by Z-stack confocal analysis. Mean podosome height ± s.d. is shown (n = 10); $P < 0.001$ by Student's t-test. *E*, Transwell migration assays were performed on the control cell line and Tm-4 overexpressers. The relative motilities are expressed as the mean of four experiments ± s.d.; $P < 0.001$ by Student's t-test.

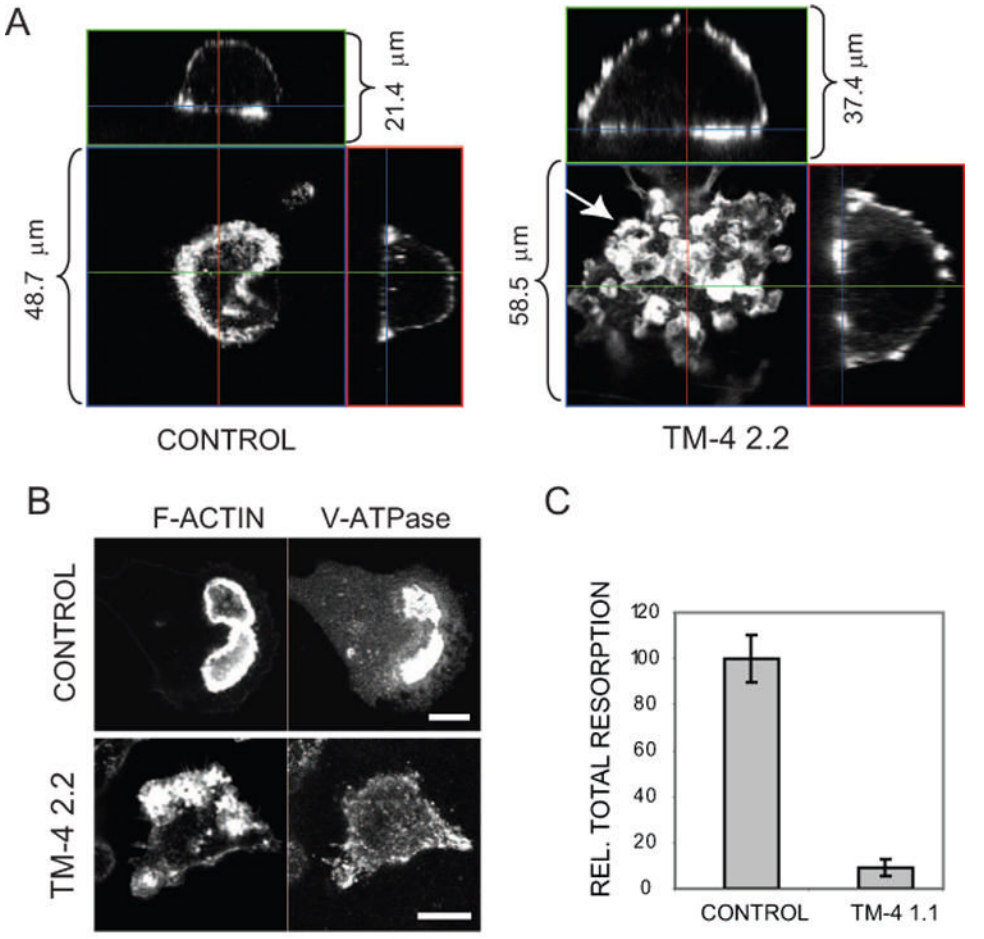

Figure 5. Overexpression of Tm-4 results in loss of the sealing zone and diminished resorptive capacity

A, Z-stack confocal analysis was performed on a control cell line (left panel) and a Tm-4 overexpresser stained for F-actin (right panel). Overexpressing cells were unable to form distinct sealing zones, although some cells demonstrated small actin ring structures (arrow). *B*, V-ATPase subunit a3 staining was performed on control-transfected and Tm-4 overexpressing cells. Unlike control cells, overexpressers did not demonstrate V-ATPase staining typical of ruffled borders. *C*, Control-transfected and Tm-4 overexpressing cells were cultured on Osteologic discs for eight days and total resorption was quantified. Shown are mean resorption ± s.d; n = 4; $P < 0.001$ by Student's t-test.